A&A 585, L3 (2016)
DOI: 10.1051/0004-6361/201527258

Astronomy & Astrophysics

Letter to the Editor

Weak-lensing *B*-modes as a probe of the isotropy of the universe

Thiago S. Pereira[1], Cyril Pitrou[2,3], and Jean-Philippe Uzan[2,3]

[1] Departamento de Física, Universidade Estadual de Londrina, 86051-990 Londrina, Paraná, Brazil
e-mail: tspereira@uel.br
[2] Institut d'Astrophysique de Paris, Université Pierre & Marie Curie – Paris VI, CNRS-UMR 7095, 98bis Bd Arago, 75014 Paris, France
[3] Sorbonne Universités, Institut Lagrange de Paris, 98bis boulevard Arago, 75014 Paris, France
e-mail: [pitrou; uzan]@iap.fr

Received 26 August 2015 / Accepted 1 December 2015

ABSTRACT

Aims. We use the angular power spectrum of *B*-modes of the weak-lensing shear as a tool for constraining late-time deviations of spatial isotropy in our Universe.
Methods. We used the formalism of weak lensing in arbitrary spacetimes.
Results. We find that off-diagonal correlations must exist between *E*-modes, *B*-modes, and convergence of the weak-lensing field, which allow one to reconstruct the eigendirections of anisotropic expansion. Focusing on future surveys, such as Euclid and the Square Kilometer Array (SKA), we find that observations can constrain the geometrical shear in units of the Hubble rate at the percent level or better. These observations offer a new and powerful method to probe our cosmological model, however, the power of this new technique still requires further investigations and a full analysis of signal-to-noise ratio.

Key words. gravitational lensing: weak – dark energy – cosmological parameters – large-scale structure of Universe – cosmology: theory

1. Introduction

According to the standard lore (Mellier 1999; Bartelmann & Schneider 2001; Peter & Uzan 2013; Stebbins 1996), in a homogeneous and isotropic background spacetime, weak lensing by the large-scale structure of the universe induces a shear field which, to leading order, only contains E-modes. The level of B-modes is used as an important sanity check during the data processing. On small scales, B-modes arise from intrinsic alignments (Crittenden et al. 2001, 2002), Born correction, lens-lens coupling (Hilbert et al. 2009; Cooray & Hu 2002), and gravitational lensing due to the redshift clustering of source galaxies (Schneider et al. 2002). On large angular scales in which the linear regime holds, it has been demonstrated (Pitrou et al. 2013) that nonvanishing B-modes would be a signature of a deviation from the isotropy of the expansion; these modes are generated by the coupling of the background Weyl tensor to the E-modes.

In this letter, we emphasize that as soon as local isotropy ceases to hold at the background level, there exists a series of weak-lensing observables that allow one to fully reconstruct the background shear and, thus, test the spatial isotropy of the universe. We also quantify their magnitude for typical surveys such as Euclid (Laureijs et al. 2011) and SKA (Garrett et al. 2010; Schneider 1999). As a consequence of the existence of B-modes, it can be demonstrated that: (1) the angular correlation function of the B-modes, C_ℓ^{BB}, is nonvanishing (Pitrou et al. 2013); (2) they also correlate with both the E-modes and the convergence κ, leading to the off-diagonal cross-correlations $\langle B_{\ell m}E^\star_{\ell\pm1\,m-M}\rangle$ and $\langle B_{\ell m}\kappa^\star_{\ell\pm1\,m-M}\rangle$ in which $E_{\ell m}$ and $B_{\ell m}$ are the components of the decomposition of the E- and B-modes of the cosmic shear in (spin-2) spherical harmonics, and $\kappa_{\ell m}$ are the components of the decomposition of the convergence in spherical harmonics (Pitrou et al. 2015); (3) late-time deviations from isotropy also generate off-diagonal correlations between κ and E-modes, $\langle E_{\ell m}E^\star_{\ell\pm2\,m-M}\rangle$, $\langle \kappa^X_{\ell m}\kappa^{X\star}_{\ell\pm2\,m-M}\rangle$, and $\langle E^X_{\ell m}\kappa^{X\star}_{\ell\pm2\,m-M}\rangle$.

Our companion article (Pitrou et al. 2015) provides all the technical details of the theoretical computation of these correlators. In this letter, we estimate the information that can be extracted from weak lensing by focusing on these correlations and illustrate its power to constrain late-time deviations of spatial isotropy.

2. Formalism

We assume that the background spacetime is spatially flat and homogeneous, but enjoys an anisotropic expansion. Such spacetime can be described by a Bianchi I universe with the following metric

$$\mathrm{d}s^2 = -\mathrm{d}t^2 + a(t)^2\gamma_{ij}(t)\mathrm{d}x^i\mathrm{d}x^j, \tag{1}$$

where $a(t)$ is the volume-averaged scale factor and latin indices run from 1 to 3. The spatial metric γ_{ij} is decomposed as $\gamma_{ij}(t) = \exp[2\beta_i(t)]\delta_{ij}$ with the constraint $\sum_{i=1}^3\beta_i = 0$. The geometrical shear, not to be confused with the cosmic shear, is defined as

$$\sigma_{ij} \equiv \frac{1}{2}\dot{\gamma}_{ij}. \tag{2}$$

Its amplitude, $\sigma^2 \equiv \sigma_{ij}\sigma^{ij} = \sum_{i=1}^3\dot{\beta}_i^2$, characterizes the deviation from a Friedmann-Lemaître spacetime. We define the rate of expansion as usual: $H = \dot{a}/a$.

At this stage, it is important to stress that, since σ_{ij} is traceless, it has five independent components. In the limit in which $\sigma/H \ll 1$ (the relevant limit to constrain small departures from isotropic expansion) each of the five correlators, i.e.,

$\langle B_{\ell m}E^{\star}_{\ell\pm1\,m-M}\rangle$, $\langle B_{\ell m}\kappa^{\star}_{\ell\pm1\,m-M}\rangle$, $\langle E_{\ell m}E^{\star}_{\ell\pm2\,m-M}\rangle$, $\langle \kappa^{X}_{\ell m}\kappa^{X\star}_{\ell\pm2\,m-M}\rangle$, and $\langle E^{X}_{\ell m}\kappa^{X\star}_{\ell\pm2\,m-M}\rangle$, is of first order in σ/H and has five independent components ($M = -2\ldots+2$) that allow one, in principle, to reconstruct the independent components of σ_{ij}. The angular power spectrum C^{BB}_{ℓ}, on the other hand, scales as $(\sigma/H)^2$ and, while it can point to a deviation from isotropy, it does not allow one to reconstruct the principal axis of expansion.

Following our earlier works (Pitrou et al. 2013, 2015), we adopt an observer-based point of view, i.e., we compute all observable quantities in terms of the direction of observation $\boldsymbol{n}_{\rm o}$. The main steps of the computation are: (1) the resolution of the background geodesic equation, which provides the local direction $\boldsymbol{n}(\boldsymbol{n}_{\rm o}, t)$ on the lightcone and, hence, the definition of the local Sachs basis; (2) the resolution of the Sachs equation at the background level and at linear order in perturbations; and (3) a multipole decomposition of all the quantities, which is a step more difficult than usual because of the fact that $\boldsymbol{n} \neq \boldsymbol{n}_{\rm o}$. We then perform a small shear limit expansion in which one can isolate the dominant terms, followed by the use of the Limber approximation (although this approximation is not mandatory). This program gives the expressions of the different correlators

$$
\begin{aligned}
{}^{XZ}\mathcal{A}^{M}_{\ell_1\ell_2} \equiv & \sum_m \sqrt{5}(-1)^{m+\ell_1+\ell_2}\begin{pmatrix} \ell_1 & 2 & \ell_2 \\ -m & M & m-M \end{pmatrix}, \\
& \times \langle X^{X}_{\ell_1 m} Z^{X\star}_{\ell_2, m-M}\rangle
\end{aligned} \tag{3}
$$

which take the form (see Eqs. (7.17)–(7.19) of Pitrou et al. 2015)

$$
\begin{aligned}
{}^{BE}\mathcal{A}^{M}_{\ell\ell\pm1} &= \mathrm{i}\frac{{}_2F_{\ell 2\ell\pm1}}{\sqrt{5}}\,\mathcal{P}^{EE}_{\ell\pm1M}, \\
{}^{B\kappa}\mathcal{A}^{2M}_{\ell\ell\pm1} &= \mathrm{i}\frac{F_{\ell 2\ell\pm1}}{\sqrt{5}}\,\mathcal{P}^{E\kappa}_{\ell\pm1M}, \\
{}^{EE}\mathcal{A}^{M}_{\ell\ell\pm2} &= \frac{{}_2F_{\ell 2\ell\pm2}}{\sqrt{5}}\,\mathcal{P}^{EE}_{\ell\pm2M} + \frac{{}_2F_{\ell\pm22\ell}}{\sqrt{5}}\mathcal{P}^{EE}_{\ell M}, \\
{}^{\kappa\kappa}\mathcal{A}^{M}_{\ell\ell\pm2} &= \frac{F_{\ell 2\ell\pm2}}{\sqrt{5}}\,\mathcal{P}^{\kappa\kappa}_{\ell\pm2M} + \frac{F_{\ell\pm22\ell}}{\sqrt{5}}\mathcal{P}^{\kappa\kappa}_{\ell M}, \\
{}^{E\kappa}\mathcal{A}^{M}_{\ell\ell\pm2} &= \frac{{}_2F_{\ell 2\ell\pm2}}{\sqrt{5}}\,\mathcal{P}^{E\kappa}_{\ell\pm2M} + \frac{F_{\ell\pm22\ell}}{\sqrt{5}}\,\mathcal{P}^{\kappa E}_{\ell M}.
\end{aligned}
$$

Here, ${}_sF_{\ell_1 2\ell_2}$ are explicit functions of the multipoles given in the Appendix of Pitrou et al. (2015) and defined in Hu (2000). The general form of the quantities $\mathcal{P}^{XY}_{\ell m}$ are found in Pitrou et al. (2015) and, in the Limber approximation, they reduce to

$$
\begin{bmatrix} \mathcal{P}^{\kappa\kappa}_{\ell M} \\ \mathcal{P}^{\kappa E}_{\ell M} \\ \mathcal{P}^{EE}_{\ell M} \end{bmatrix} = \frac{1}{4}\begin{bmatrix} \ell^2(\ell+1)^2 \\ \ell(\ell+1)\sqrt{\frac{(\ell+2)!}{(\ell-2)!}} \\ \frac{(\ell+2)!}{(\ell-2)!} \end{bmatrix} \times \mathcal{P}_{\ell M}, \tag{4}
$$

with (see Eqs. (7.20) and (7.21) of Pitrou et al. 2015)

$$
\begin{aligned}
\mathcal{P}_{\ell M} \equiv & \int_0^\infty \frac{\mathrm{d}\tilde\chi}{\tilde\chi^2} P\left(\frac{L}{\tilde\chi}\right)\alpha_{2M}(\tilde\chi) \\
& \times \left| T^{\varphi}\left(\frac{L}{\tilde\chi}, \tilde\chi\right) \int_{\tilde\chi}^{\infty} \mathrm{d}\chi\; N(\chi)\frac{(\chi-\tilde\chi)}{\chi\tilde\chi}\right|^2,
\end{aligned} \tag{5}
$$

and $L \equiv \ell + 1/2$. Here, $P(k)$ stands for the primordial power spectrum of the metric fluctuations, $T^{\varphi}(x,\eta)$ is the transfer function of the deflecting potential given, as usual, by the sum of the two Bardeen potentials. They are both evaluated on the past lightcone parametrized by the radial coordinate χ; in the Limber approximation, $k = L/\tilde\chi$. $N(\chi)$ is the source distribution and depends on the details of the specific survey. The quantity $\alpha_{\ell m}(\chi)$ is the multipolar coefficient of the deflection angle $\alpha(\boldsymbol{n}_{\rm o}, \chi)$ expanded in spherical harmonics. At the lowest order in σ/H, only its $\ell = 2$ components are nonvanishing. (See Sect. VII.B.2 of Pitrou et al. 2015 for the expressions of α_{2m}.)

While the previous off-diagonal correlators are the most direct consequence of a late-time anisotropy, most experiments are designed to measure the angular power spectrum. We obtain (Pitrou et al. 2015) for the B-modes,

$$
\begin{aligned}
C^{BB}_{\ell} = & \frac{2}{5\pi}\int_0^\infty k^2\mathrm{d}k P(k)\sum_{s=\pm1}\frac{({}_2F_{\ell 2\ell+s})^2}{2\ell+1} \\
& \times \sum_m \left| \int_0^\infty \mathrm{d}\chi N(\chi)\int_0^\chi \mathrm{d}\chi' \alpha_{2m}(\chi') g^{E}_{\ell+s}(k,\chi,\chi')\right|^2,
\end{aligned} \tag{6}
$$

where ${}_2F_{\ell 2\ell+s}$ is a function of ℓ and s, and the functions g^{E}_{ℓ} are expressed in terms of spherical Bessel functions, given by Eq. (6.44) of Pitrou et al. (2015).

To estimate these correlators, we carry out the following steps. First, we need to solve the geodesic equation for the background spacetime to determine $\boldsymbol{n}(\boldsymbol{n}_0, \chi)$ and the deflection angle. We then need to describe and solve the evolution of metric perturbations (to determine the transfer function T^{φ} of the lensing potential).

3. Observational constraints

During inflation, the spacetime isotropizes, letting only tiny, if any, signatures on the cosmic microwave background (CMB; Pereira et al. 2007; Pitrou et al. 2008), which has been constrained observationally (Maartens et al. 1995; Eriksen et al. 2004; Jaffe et al. 2005; Hoftuft et al. 2009; Akrami et al. 2014; Campanelli et al. 2007; Battye & Moss 2009; Planck Collaboration XVI 2015). On the other hand, many models of the dark sector (Bucher & Spergel 1999; Battye & Moss 2005; Mota et al. 2007; Koivisto & Mota 2008b; Sharif & Zubair 2010) have considered the possibility that dark energy enjoys an anisotropic stress. This is a generic prediction of bigravity (Damour et al. 2002) and backreaction (Marozzi & Uzan 2012), which has stimulated the investigation of methods to constrain a late-time anisotropy with, for example, the integrated Sachs-Wolfe effect (Campanelli et al. 2007; Battye & Moss 2009), large-scale structure, and the Hubble diagram of supernovae in different fields (Fleury et al. 2015; Saunders 1968; Appleby et al. 2010, 2015; Cai & Tuo 2012; Schucker et al. 2014; Appleby & Shafieloo 2014; Yoon et al. 2014).

From a phenomenological point of view, one can consider a dark energy sector with an anisotropic stress. Its stress-energy tensor is then decomposed as $T^{\mu}_{\nu} = (\rho+P)u^{\mu}u_{\nu} + P\delta^{\mu}_{\nu} + \Pi^{\mu}_{\nu}$, where the anisotropic stress tensor Π^{μ}_{ν} is traceless ($\Pi^{\mu}_{\mu} = 0$), transverse ($u_{\mu}\Pi^{\mu}_{\nu} = 0$), and has five degrees of freedom encoded in its spatial part Π^{i}_{j}. This can be decomposed in terms of an anisotropic equation of state (Koivisto & Mota 2008a; Appleby & Linder 2013) as $P^{j}_{i} = \rho_{\rm de}\left(w\delta^{j}_{i} + \Delta w^{j}_{i}\right)$. Here, w is the usual equation of state (we assume $w = -1$ as for a cosmological constant) and we need to model Π^{i}_{j}. The background equations then take the form

$$
\begin{aligned}
3H^2 &= 8\pi G(\rho_{\rm m} + \rho_{\rm de}) + \frac{1}{2}\sigma^2, && (7)\\
(\sigma^{i}_{\ j})^{\cdot} &= -3H\sigma^{i}_{\ j} + 8\pi G\Pi^{i}_{j}. && (8)\\
\dot\rho_{\rm m} &= -3H\rho_{\rm m}, && (9)\\
\dot\rho_{\rm de} &= -\sigma_{ij}\Pi^{ij}. && (10)
\end{aligned}
$$

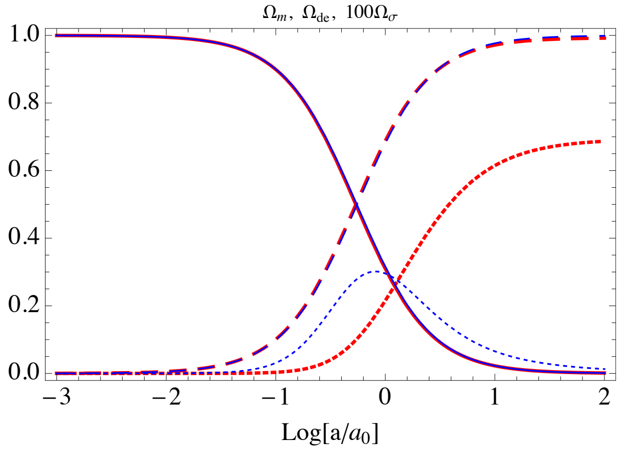

Fig. 1. Time evolution of models A (red) and B (blue). The plot shows the contribution to the expansion of matter (solid line), dark energy (dashed line), and geometrical shear (dotted line, and magnified by a factor 100).

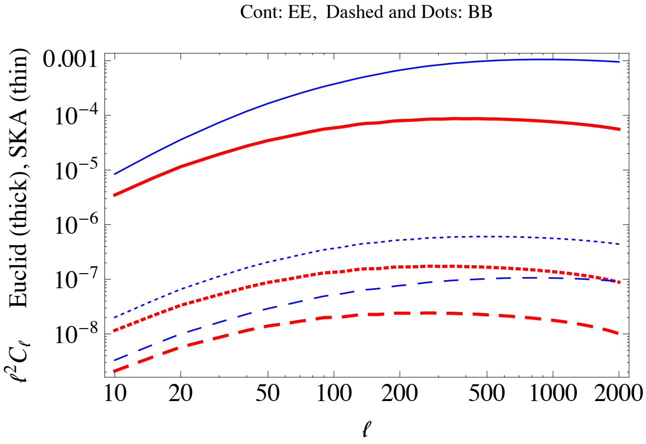

Fig. 2. Angular power spectra of the E- and B-modes (resp. solid and dashed lines) for the Euclid (red lines) and SKA (blue lines) surveys for models A (long dashed) and B (short dashed).

The first equation is the equivalent of the Friedmann equation, and the second is obtained from the traceless and transverse part of the Einstein equation and dictates the evolution of the shear. The last two equations are the continuity equations for the dark matter ($P = \Pi^i_j = 0$) and dark energy sectors.

Simple models can be built by phenomenologically relating Π^i_j to the geometrical shear as $\Pi^i_j = \lambda\sigma^i_j \equiv \sigma^i_j/(8\pi G\tau_\Pi)$, where τ_Π can be time dependent. When the shear is constant, it grows exponentially as $\sigma^i_j = B^i_j\left(\frac{a_0}{a}\right)^3 \mathrm{e}^{t/\tau_\Pi}$. Since σ_{ij} is small today, there is some fine-tuning. We thus consider two classes of models defined by

$$(A):\quad \Pi^i_j \equiv \rho_{\rm de}\Delta w^i_j\,;\qquad (B):\quad \Pi^i_j \equiv g(a)\Delta w^i_j. \tag{11}$$

This assumes that the anisotropic stress evolves with time, while keeping its eigenvalues in a constant ratio. The function $g(a)$ is arbitrary and when $g(a) = 3H/H_0$, $\sigma^i_j = C^i_j\left(\frac{a_0}{a}\right)^3 + 8\pi G\frac{\Delta w^i_j}{H_0}$; hence, at late time $\sigma^2 \propto \Delta w^2/H_0^2$ is constant. In the models (A), the dark energy triggers the anisotropic phase. It has been argued (Appleby & Linder 2013) that next generation surveys will be capable of constraining anisotropies at the 5% level in terms of the anisotropic equation of state, which is a number to keep in mind for comparison with weak lensing.

Moving forward, Eq. (8) implies that

$$\sigma^i_j = \left(\frac{a_0}{a}\right)^3\left[C^i_j + \kappa\int \Pi^i_j\left(\frac{a}{a_0}\right)^2\frac{\mathrm{d}(a/a_0)}{H}\right],$$

while Eq. (10) implies that $\rho_{\rm de}$ decreases as

$$\rho_{\rm de} = \rho_{\rm de0}\exp\left[-\int \sigma^j_i \Delta w^i_j \frac{\mathrm{d}a}{aH}\right].$$

Figure 1 depicts the evolution of the density parameters for a model of each class.

To evaluate the angular power spectrum of the E- and B-modes, one needs to specify $\mathcal{N}(\chi)$. To this end, we consider the distributions of the future Euclid and SKA experiments. The normalized Euclid redshift distribution (Beynon et al. 2010; Laureijs et al. 2011) is

$$\mathcal{N}(z) = Az^2\exp\left[-\left(\frac{z}{z_0}\right)^\beta\right], \tag{12}$$

with $A = 5.792$, $\beta = 1.5$ and $z_0 = 0.64$. For SKA, we use the SKA Simulated Skies simulations (Wilman et al. 2008) of the radio source population with the extragalactic radio continuum sources in the central 10×10 sq. deg up to $z = 20$. The SKA normalized redshift distribution is (Andrianomena et al. 2014)

$$\mathcal{N}(z) = A\frac{z^n}{(1+z)^m}\exp\left[-\frac{(a+bz)^2}{(1+z)^2}\right],\qquad z < 20 \tag{13}$$

with best-fit parameters $a = -1.806, b = 0.388, m = 2.482, n = 0.838$, and $A = 1.610$, which yield a description that is accurate to the percent level.

Figure 2 depicts the two angular power spectra for these two surveys. In the linear regime, the B-mode contribution is expected to vanish and the terms $\ell^4\mathcal{P}_{\ell M}$, proportional to the off-diagonal correlators ${}^{XY}\!\mathcal{A}^M_{\ell\ell\pm1}$, are shown in Fig. 3. However, the shear induces a B-mode spectrum whose amplitude is about $(\sigma/H)^2$ lower than for the E-mode spectrum in the most optimistic model (B). We can compare our results to the bounds set by the CFHTLS survey (Kitching et al. 2014). Unfortunately, CFHTLS covers four fields of typical size 50 sq. deg so that the largest scale with a sufficiently good signal-to-noise ratio is on the order of $\ell \sim 2000$, which is far beyond the linear regime. The B-modes are generated from nonlinear dynamics and it is safer to rely on the EB cross-correlation. To get a rough idea, however, we use the values at $\ell = 2000$, for which $\ell^2 C^{EE}_\ell \sim 10^{-6}$ and $\ell^2 C^{EB}_\ell < 4\times10^{-7}$. Indeed, this estimate has to be taken with a grain of salt given the fact that *i)* there is a large scatter in Figs. 6 and 7 of Kitching et al. (2014); and *ii)* these observations are not in the linear regime and there is no unambiguous way to scale these observations to lower ℓ. We can thus set the bound $(\sigma/H)_0 \lesssim 0.4$ from CFHTLS. However, Euclid shall probe scales up to 100 deg, deep in the linear regime, with a typical improvement of a factor 50 (Mellier 2015, priv. comm.). This would translate to a sensitivity of order $(\sigma/H)_0 \lesssim 0.4/50 \sim 1\%$ for the shear. This estimate indicates that weak lensing could be a powerful tool to constrain a late-time anisotropy. In the meantime, experiments such as DES will allow us to forecast the power of Euclid more precisely. These experiments demonstrate that in principle one can reconstruct the principle axis of expansion from observations. We thus want to draw attention to the importance of these estimators and their measurements.

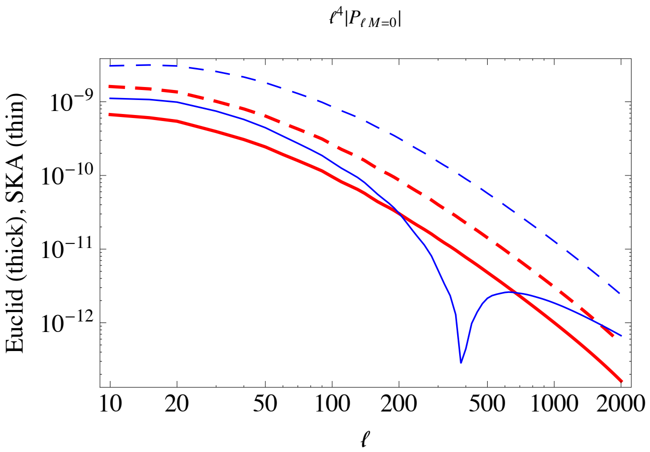

Fig. 3. The five correlators ${}^{XY}\mathcal{A}^{M}_{\ell\ell\pm1}$ are, up to shape factors, proportional to $\ell^4\mathcal{P}_{\ell M}$. We plot the latter for the models A (dashed) and B (solid) for the Euclid (red) and SKA (blue). For clarity, we only plot the $M = 0$ component.

4. Conclusions

This letter emphasises the specific signatures of an anisotropic expansion on weak lensing, as first pointed out in (Pitrou et al. 2013). Following our formalism detailed in Pitrou et al. (2015, where all the technical details can be found), we have focused on two phenomenological anisotropic models and computed the angular power spectra of the E- and B-modes and the five nonvanishing, off-diagonal correlators. These are new observables that we think must be measured in future surveys. These measurements can be combined easily with the Hubble diagram since the Jacobi matrix can be determined analytically at background level (Fleury et al. 2015). We emphasize that the off-diagonal correlations with the polarization can also be applied to the analysis of the CMB, hence, easily generalizing those built from the temperature alone (Kumar et al. 2015; Joshi et al. 2012; Abramo & Pereira 2010; Prunet et al. 2005; Fabre et al. 2015).

Our analysis demonstrates that future surveys, and in particular Euclid, can set strong bounds on the anisotropy of the Hubble flow, typically at the level of $(\sigma/H)_0 \leq 1\%$. However, one needs a detailed analysis of the signal-to-noise ratio to confirm this number, which for now has to be taken as an indication. This is a new and efficient method and the estimators built from the off-diagonal correlators can be used to reconstruct the proper axis of the expansion.

Acknowledgements. We thank Pierre Fleury and Yannick Mellier for discussions. This work was made in the ILP LABEX (under reference ANR-10-LABX-63) and was supported by French state funds managed by the ANR within the Investissements d'Avenir programme under reference ANR−11−IDEX−0004−02, the Programme National Cosmologie et Galaxies, and the ANR THALES (ANR-10-BLAN-0507-01-02). Thiago Pereira thanks Conselho Nacional de Desenvolvimento Científico e Tecnológico (CNPq) for its financial support.

References

Abramo, L. R., & Pereira, T. S. 2010, Adv. Astron., 2010, 378203
Akrami, Y., Fantaye, Y., Shafieloo, A., et al. 2014, ApJ, 784, L42
Andrianomena, S., Clarkson, C., Patel, P., Umeh, O., & Uzan, J.-P. 2014, JCAP, 1406, 023
Appleby, S. A., & Linder, E. V. 2013, Phys. Rev. D, 87, 023532
Appleby, S., & Shafieloo, A. 2014, JCAP, 1410, 070
Appleby, S., Battye, R., & Moss, A. 2010, Phys. Rev. D, 81, 081301
Appleby, S., Shafieloo, A., & Johnson, A. 2015, ApJ, 801, 76
Bartelmann, M., & Schneider, P. 2001, Phys. Rept., 340, 291
Battye, R. A., & Moss, A. 2005, JCAP, 0506, 001
Battye, R., & Moss, A. 2009, Phys. Rev. D, 80, 023531
Beynon, E., Bacon, D. J., & Koyama, K. 2010, MNRAS, 403, 353
Bucher, M., & Spergel, D. N. 1999, Phys. Rev. D, 60, 043505
Cai, R.-G., & Tuo, Z.-L. 2012, JCAP, 1202, 004
Campanelli, L., Cea, P., & Tedesco, L. 2007, Phys. Rev. D, 76, 063007
Cooray, A., & Hu, W. 2002, ApJ, 574, 19
Crittenden, R. G., Natarajan, P., Pen, U.-L., & Theuns, T. 2001, ApJ, 559, 552
Crittenden, R. G., Natarajan, P., Pen, U.-L., & Theuns, T. 2002, ApJ, 568, 20
Damour, T., Kogan, I. I., & Papazoglou, A. 2002, Phys. Rev. D, 66, 104025
Eriksen, H. K., Hansen, F. K., Banday, A. J., Gorski, K. M., & Lilje, P. B. 2004, ApJ, 605, 14; Erratum: ApJ, 609, 1198
Fabre, O., Prunet, S., & Uzan, J.-P. 2015, Phys. Rev. D, 92, 043003
Fleury, P., Pitrou, C., & Uzan, J.-P. 2015, Phys. Rev. D, 91, 043511
Garrett, M. A., Cordes, J. M., Deboer, D. R., et al. 2010, PoS, ISKAF2010, 018
Hilbert, S., Hartlap, J., White, S. D. M., & Schneider, P. 2009, A&A, 499, 31
Hoftuft, J., Eriksen, H. K., Banday, A. J., et al. 2009, ApJ, 699, 985
Hu, W. 2000, Phys. Rev. D, 62, 043007
Jaffe, T. R., Banday, A. J., Eriksen, H. K., Gorski, K. M., & Hansen, F. K. 2005, ApJ., 629, L1
Joshi, N., Rotti, A., & Souradeep, T. 2012, Phys. Rev. D, 85, 043004
Kitching, T. D., Heavens, A. F., Alsing, J., et al. 2014, MNRAS, 442, 1326
Koivisto, T., & Mota, D. F. 2008a, ApJ, 679, 1
Koivisto, T., & Mota, D. F. 2008b, JCAP, 0806, 018
Kumar, S., Rotti, A., Aich, M., et al. 2015, Phys. Rev. D, 91, 043501
Laureijs, R., Amiaux, S., Arduini, J.-L., et al. 2011, ArXiv e-prints [arXiv:1110.3193]
Maartens, R., Ellis, G. F. R., & Stoeger, W. R. 1995, Phys. Rev. D, 51, 5942
Marozzi, G., & Uzan, J.-P. 2012, Phys. Rev. D, 86, 063528
Mellier, Y. 1999, ARA&A, 37, 127
Mota, D. F., Kristiansen, J. R., Koivisto, T., & Groeneboom, N. E. 2007, MNRAS, 382, 793
Pereira, T. S., Pitrou, C., & Uzan, J.-P. 2007, JCAP, 0709, 006
Peter, P., & Uzan, J.-P. 2013, Primordial cosmology (Oxford University Press)
Pitrou, C., Pereira, T. S., & Uzan, J.-P. 2008, JCAP, 0804, 004
Pitrou, C., Uzan, J.-P., & Pereira, T. S. 2013, Phys. Rev. D, 87, 043003
Pitrou, C., Pereira, T. S., & Uzan, J.-P. 2015, Phys. Rev. D, 92, 023501
Prunet, S., Uzan, J.-P., Bernardeau, F., & Brunier, T. 2005, Phys. Rev. D, 71, 083508
Planck Collaboration XVI. 2015, A&A, submitted [arXiv:1506.07135]
Saunders, P. 1968, MNRAS, 141, 427
Schneider, P. 1999, ArXiv e-prints [arXiv:astro-ph/9907146]
Schneider, P., Waerbeke, L. V., & Mellier, Y. 2002, A&A, 389, 729
Schucker, T., Tilquin, A., & Valent, G. 2014, MNRAS, 444, 2820
Sharif, M., & Zubair, M. 2010, Astrophys. Space Sci., 330, 399
Stebbins, A. 1996, ArXiv e-prints [arXiv:astro-ph/9609149]
Wilman, R. J., Miller, L., Jaruis, M. J., et al. 2008, MNRAS, 388, 1335
Yoon, M., Huterer, D., Gibelyou, C., Kovàcs, A., & Szapudi, I. 2014, MNRAS, 445, L60